Bearing capacity prediction of inclined loaded strip footing on reinforced sand by ANN

R Sahu[1], C R Patra[2], N Sivakugan[3], B M Das[4]

[1]Research Scholar, National Institute of Technology, Rourkela, India, email: roma.sahu.civ@gmail.com
[2]Professor, National Institute of Technology, Rourkela, India, email: crpatra19@yahoo.co.in
[3]Associate Professor, James Cook University, Townsville, Australia, email: siva.sivakugan@jcu.edu.in
[4]Dean Emeritus, California State University, Sacramento, USA, email: brajamdas@gmail.com

ABSTRACT: Laboratory model tests have been conducted on a strip foundation resting over multi-layered geogrid-reinforced dense and loose sand subjected to inclined load. Based on the laboratory model test results, a neural network model is developed to estimate the reduction factor for bearing capacity. The reduction factor obtained by ANN can be used to estimate the ultimate bearing capacity of an inclined loaded foundation from the ultimate bearing capacity of a vertically loaded foundation. A thorough sensitivity analysis was carried out to find out the important parameters affecting the reduction factor. Emphasis was given on the construction of neural interpretation diagram, based on the weights developed in the neural network model, to determine the direct or inverse effect of input parameters to the output. An ANN model equation is developed based on trained weights of the neural network model. The results from artificial neural network (ANN) were compared with the laboratory model test results and these results are in good agreement.

Keywords: *Inclined load, Geogrid, Sand, Neural network, Ultimate bearing capacity, Reduction factor.*

INTRODUCTION

During the last thirty years, a number of laboratory model test results and few field test results have been published that are related to the ultimate bearing capacity of shallow foundation resting over geogrid reinforced sand and clay. Most of the experimental studies were related to centric loading condition. However, none of the published studies address the effect of load inclination on the ultimate bearing capacity of strip foundation resting over multi-layered geogrid reinforced sand. The purpose of this study is to develop a neural network model from the results of laboratory model tests conducted by Sahu *et al*. (2016) to estimate the reduction factor. This *RF* is the ratio of the ultimate bearing capacity of strip footing on reinforced sand subjected to an inclined load to the ultimate bearing capacity of footing subjected to a centric vertical load at the same depth of embedment. In the present study, a feed-forward back-propagation neural network is trained with Levenberg-Marquardt algorithm. A thorough sensitivity analysis is made to interpret the important input variables. Neural Interpretation diagram is constructed based on the weights of the developed neural network model, to determine whether the input parameters have direct or inverse effect on the output. A prediction model equation is developed based on the weights of the neural network model. The predicted reduction factor is compared with the empirical equation proposed by Sahu *et al*. (2016).

DATABASE AND PREPROCESSING

The extensive database of laboratory experimental data available in Sahu *et al*. (2016) has been employed in the present study. Load tests were carried out on model strip footings resting on geogrid reinforced sand subjected to inclined loads as shown in FIG. 1. The details of the tests and the procedure have been described in Sahu *et al*. (2016). The database used in the present analysis is presented in Table 1. The database consist of parameters like load inclination α, embedment ratio D_f /B, depth of reinforcement measured from the bottom of the foundation d, friction angle ϕ and ultimate bearing capacity q_{uR}. Eighty laboratory model tests were conducted. α/ϕ and d_f /B are used as the two dimensionless input parameters in the ANN model and the output is the reduction factor (*RF*). The reduction factor (*RF*) is given by

$$RF = \frac{q_{uR(\alpha/\phi,\, d_f/B)}}{q_{uR(\alpha/\phi=0,\, d_f/B)}} \tag{1}$$

where $q_{uR(\alpha/\phi, d_f/B)}$ is the ultimate bearing capacity with inclination ratio α/ϕ at an normalized depth of reinforcement layer ratio d_f/B and $q_{uR(\alpha/\phi=0, d_f/B)}$ is the ultimate bearing capacity with centric vertical loading (i.e. $\alpha/\phi = 0$) at depth of reinforcement layer ratio d_f/B. In the present study, out of 80 data points 64 points were used for training and remaining 16 were kept for testing. Each data point represents a complete laboratory model test on geogrid reinforced bed which was led to failure. All the inputs and output are normalized in the range of [-1, 1] before training. A feed-forward back-propagation neural network is used with hyperbolic tangent sigmoid function and linear function as the transfer function. The network is trained with Levenberg-Marquardt (LM) algorithm as it is efficient in comparison to gradient descent back-propagation algorithm. The ANN has been implemented using MATLAB V 7.11.0(R2015b).

RESULTS AND DISCUSSION

Two inputs and one output parameters were considered in the ANN model. The maximum, minimum, average and standard deviation values of the two input and one output parameters used in the ANN model are presented in Table 2.

The schematic diagram of ANN architecture is shown in FIG. 2. The number of neurons in hidden layer is varied and it was selected based on the mean square error (MSE) value which was 0.001. In this ANN model four neurons are evaluated in hidden layer as shown in FIG. 3. Therefore the final ANN architecture is retained as 2-4-1 [i.e. 2 (input) – 4 (hidden layer neuron) – 1 (output)]. Mean square error (MSE) is defined as

$$MSE = \frac{\sum_{i=1}^{n}\left(RF_i - RF_p\right)^2}{n} \tag{2}$$

Coefficient of efficiency, R^2 is defined as

$$R^2 = \frac{E_1 - E_2}{E_1} \tag{3}$$

where,

$$E_1 = \sum_{i=1}^{n}(RF_i - \overline{RF})^2 \tag{4}$$

and

$$E_2 = \sum_{i=1}^{n}\left(RF_P - RF_I\right)^2 \tag{5}$$

where, RF_i, $\overline{RF}$ and RF_p are the experimental, average experimental, predicted RF values respectively; and n = number of training data.

The coefficient of efficiency (R^2) is found to be 0.9972 for training and 0.9952 for testing as shown in FIG. 4 and 5. All the data used in the training and testing have been obtained from laboratory model tests are from the same source and are of same nature. Probably, this may be one of the causes for better fitting in both training and testing phase as well. The weights and biases of the network are presented in Table 3. These weights and biases can be utilized for interpretation of relationship between the inputs and output, sensitivity analysis and framing an ANN model in the form of an equation. The residual analysis was carried out by calculating the residuals in between experimental reduction factor and predicted reduction factor for training data. Residuals can be defined as the difference between the experimental and predicted RF value and is given by

$$e_r = RF_i - RF_p \tag{6}$$

The residuals are plotted with the experimental number as shown in FIG. 6. It is observed that the residuals are evenly distributed along the horizontal axis of the plot. Therefore it can be said that the network is well trained and can be used for prediction with reasonable accuracy.

SENSITIVITY ANALYSIS

Sensitivity analysis was carried out for selection of important input variables. Different approaches have been suggested to select the important input variables. Connection weight approach by Olden *et al*. (2004), Garson's algorithm approach by (Garson 1991), Pearson correlation coefficient approach by Guion and Elisseff (2003) have been applied for sensitivity analysis. The Pearson correlation coefficient is one of them in selecting proper inputs for the ANN model. Goh (1994) and Sahin *et al*. (2002) have used Garson's algorithm (Garson 1991) in which the input-hidden and hidden-output weights of trained ANN model are partitioned and the absolute values of weights are taken to select the important input variables. It does not provide information on the effect of input variables in terms of direct or inverse relation to the output. Olden *et al*. (2004) proposed a connection weights approach based on the NID, in which the actual values of input-hidden and hidden-output weights are taken. Table 4 shows the cross-correlation of inputs with the reduction factor (*RF*) value. It can be seen that *RF* is highly correlated to α/ϕ with a cross correlation value of 0.928, followed by d_f/B. From analysis of Garson's algorithm as presented in Table 5 it is seen that α/ϕ is found to be most Important input parameter with the relative importance value being 61.13% followed by 38.86% for d_f/B. Olden *et al*. (2004) proposed a connection weights approach based on the NID, in which the actual values of input-hidden and hidden-output weights are taken. It sums the products across all the hidden neurons, which is defined as S_i. The most important input corresponds to highest S_i value. As per Connection weight approach analysis it is seen that α/ϕ is found to be most important input parameter (S_i value = -11.34) followed by d_f/B (S_i value = 10.44). The S_i values being negative imply that α/ϕ is indirectly and d_f/B is directly related to *RF* values. From the sensitivity analysis it can be seen that α/ϕ is found to be the most important parameter in predicting *RF*. In other words, increasing α/ϕ will lead to a reduction in the *RF* and hence leads to lower ultimate bearing capacity. Increasing d_f/B increases the *RF*, and hence, increases the bearing capacity.

NEURAL INTERPRETATION DIAGRAM (NID)

Ozesmi and Ozesmi (1999) proposed a neural interpretation diagram (NID) for visual interpretation of the connection weight among the neurons. For the present study with the weights as obtained and shown in Table 3, an NID is presented in FIG. 7. The lines joining the input-hidden and hidden-output neurons represent the weights. The positive weights are represented by solid lines and negative weights by dashed lines and the thickness of the lines is proportional to their magnitude. The input directly related to the output is represented with a grey circle and that having inverse effect with blank circle. It can be seen from Table 5 (4th column) that S_i value for parameter α / ϕ is negative indicating that the parameters α / ϕ is inversely related to *RF* values, whereas S_i value for parameter d_f / B being positive is directly related to *RF* values. The same has been shown in FIG. 7. Thus it is inferred that *RF* value decreases with increase in α / ϕ value and increases with increase in d_f / B value.

ANN MODEL EQUATION FOR THE REDUCTION FACTOR BASED ON TRAINED NEURAL NETWORK

In the present study, with only two parameters (d_f / B and α / ϕ) a model equation is developed using the weights obtained from trained neural network model (Goh *et al*. 2005). The mathematical equation relating the input variables and the output can be written as,

$$RF_n = f_n \left\{ b_0 + \sum_{k=1}^{h} \left[w_k f_n \left(b_{hk} + \sum_{i=1}^{m} w_{ik} X_i \right) \right] \right\} \quad (7)$$

where, RF_n = normalized value of *RF* in the range [-1, 1]

f_n = transfer function

h = number of neurons in the hidden layer

X_i = normalized value of inputs in the range [-1, 1]

m = no. of input variables

w_{ik} = connection weight between i^{th} layer of input and k^{th} neuron of hidden layer

w_k = connection weight between k^{th} neuron of hidden layer and single output neuron

b_{hk} = bias at the k^{th} neuron of hidden layer

b_o = bias at the output layer.

Using the values of trained weights and biases in Table 3, a step by step procedure is written down to form a relationship in the form of a equation between the input parameters (d_f / B and α / ϕ) and the output (*RF*).

Step – 1

The input parameters were normalized in the range [-1, 1] by the following expression

$$X_n = 2\left(\frac{X_1 - X_{min}}{X_{max} - X_{min}} \right) - 1 \quad (8)$$

where, X_n = Normalized value of input parameter

X_{max} = maximum values of the input parameter

X_{min} = Minimum values of the input parameter

X1 = is the data set.

Step – 2

Calculate the normalized value of reduction factor (RF_n) using the following expression

$$A_1 = -0.1886\left(\frac{d_f}{B}\right)_n - 1.5416\left(\frac{\alpha}{\phi}\right)_n + 0.6264 \tag{9}$$

$$A_2 = 0.9381\left(\frac{d_f}{B}\right)_n + 3.8625\left(\frac{\alpha}{\phi}\right)_n + 1.6575 \tag{10}$$

$$A_3 = 13.1304\left(\frac{d_f}{B}\right)_n + 29.6581\left(\frac{\alpha}{\phi}\right)_n + 31.5729 \tag{11}$$

$$A_3 = 46.6441\left(\frac{d_f}{B}\right)_n - 2.8076\left(\frac{\alpha}{\phi}\right)_n + 3.8462 \tag{12}$$

$$B_1 = 0.5663\left(\frac{e^{A_1} - e^{-A_1}}{e^{A_1} + e^{-A_1}}\right) \tag{13}$$

$$B_2 = -0.2274\left(\frac{e^{A_2} - e^{-A_2}}{e^{A_2} + e^{-A_2}}\right) \tag{14}$$

$$B_3 = -0.2938\left(\frac{e^{A_3} - e^{-A_3}}{e^{A_3} + e^{-A_3}}\right) \tag{15}$$

$$B_4 = -0.3134\left(\frac{e^{A_4} - e^{-A_4}}{e^{A_4} + e^{-A_4}}\right) \tag{16}$$

$$C_1 = -0.2683 + B_1 + B_2 + B_3 + B_4 \tag{17}$$

$$RF_n = C_1 \tag{18}$$

Step – 3

Denormalize the RF_n value obtained from Eq. 18 to actual *RF* as

$$RF = 0.5(RF_n + 1)(RF_{max} - RF_{min}) + RF_{min} \tag{19}$$

$$RF = 0.5(RF_n + 1)(1 - 0.112) + 0.112 \tag{20}$$

where, RF_{max} = maximum value of *RF* in the database and RF_{min} = minimum value of *RF* in the database.

COMPARISON WITH EMPIRICAL EQUATION BY SAHU *ET AL*. (2016)

Sahu *et al*. (2016) proposed an empirical equation based on laboratory model tests data for prediction of *RF*, which can be expressed as

$$RF = \frac{q_{u(\alpha/\phi,\, d_f/B)}}{q_{u(\alpha/\phi=0,\ d_f/B)}} = \left[\left[1.36 - 0.45\left[\frac{D_f}{B}\right]\right]\left[\frac{d_f}{B}\right]^{\left[0.08+0.25\left[\frac{D_f}{B}\right]\right]}\left[\frac{\alpha}{\phi}\right]^{\left[0.77+0.29\left[\frac{D_f}{B}\right]\right]}\right] \tag{21}$$

where, $q_{uR(e/B,\, d_f/B)}$= Ultimate bearing capacity of geogrid reinforced sand due to inclined loading for a particular d_f/B; $q_{uR(\alpha/\phi=0,\, d_f/B)}$ = Ultimate bearing capacity of geogrid reinforced sand for $\alpha/\phi = 0$ at the same d_f/B; and *RF* = Reduction factor.

As seen in FIG. 8 and Table 1, the comparison appears to be reasonably good. Hence, artificial neural network can be effectively used for the prediction of ultimate bearing capacity of strip footing in geogrid reinforced soil under inclined load.

CONCLUSIONS

The following conclusions can be drawn from the above studies:

1. As per residual analysis, the errors are distributed evenly along the centerline. It can be concluded that the network is well trained and can predict the result with reasonable accuracy.
2. The developed ANN model could explain the physical effect of inputs on the output, as depicted in NID. It was observed that α/ϕ were inversely related to *RF* values, whereas, d_f/B was directly related to *RF*.
3. Based on sensitivity analyses; Pearson correlation coefficient, Garson's algorithm and connection weight approaches, it was observed that α/ϕ is the most important parameter.
4. An equation is presented based on the trained weights of the ANN.
5. The predictability of ANN models are found to be slightly better than the empirical equation developed by Sahu *et al*. (2016).

REFERENCES

Behera, *et.al*. (2013). Prediction of ultimate bearing capacity of eccentrically inclined loaded strip footing by ANN part 1. International Journal of Geotechnical Engineering, doi:10.1179/1938636212Z.00000000012

Das, *et.al*. (1998). Foundation on geogrid-reinforced sand-effect of transient loading. *Geotextile and Geomembrane*, doi: S0266-1144(98)00004-1

Das, *et. al*. (2004). Developments on the bearing capacity of shallow foundations on geogrid reinforced soil - a review. *Proceedings International Conference of Geotechnical. Engineering*, University of Sharjah, UAE, 20–48.

Das S.K. and Basudhar P.K. (2008). Prediction of residual friction angle of clays using artificial neural network, Engineering Geology, doi:10.1016/J.enggeo.2008.03.001

Garson, G.D. (1991). Interpreting neural-network connection weights, Artificial Intelligence Expert, 6(7), 47–51.

Goh *et.al*. (2005). Bayesian neural network analysis of undrained side resistance of drilled shafts, Journal of Geotechnical and Geoenvironmental Engineering, doi: 10.1061/(ASCE)1090 0241(2005)131:1(84)

Guido, *et.al*. (1986). Comparison of geogrid and geotextile reinforced earth slabs. *Canadian Geotechnical Journal*, doi:10.1139/t86-073

Guyon I. and Elisseeff A. (2003). An introduction to variable and feature selection, Journal of Machine Learning Research, 3, 1157–1182.

Ozesmi S.L. and Ozesmi U. (1999). An artificial neural network approach to spatial modeling with inter specific interactions, Ecological Modelling, doi: S0304 3800(98)00149-5

Olden, *et.al*. (2004). An accurate comparison of methods for quantifying variable importance in artificial neural networks using simulated data, Ecological. Modelling, 178, (3), 389–397.

Shahin, *et. al*. (2002). Predicting settlement of shallow foundations using neural network. Journal of Geotechnical and Geoenvironmental Enigennering. doi: 10.1061/(ASCE)1090 0241(2002)128:9(785)

Sahu, *et. al*. (2016). Bearing capacity of shallow strip foundation on geogrid-reinforced sand subjected to inclined load. doi:10.1080/19386362.2015.1105622

Table 1. Database used for ANN model and comparison with Sahu *et al*. (2016)

Data type (1)	**Expt. No. (2)**	d_f/B **(3)**	(α/ϕ) **(4)**	**Experimental q_u (kN/m²) (5)**	**RF(expt) (6)**	**RF(ANN) (7)**	**RF(Pred) (8)**
Training	1	0.350	0.122	208	0.754	0.754	0.752
	2	0.350	0.244	159	0.576	0.595	0.578
	3	0.350	0.367	116	0.420	0.415	0.423
	4	0.350	0.489	74	0.268	0.258	0.279
	5	0.600	0.000	370	1.000	1.000	1.000
	6	0.600	0.122	272	0.735	0.719	0.741
	7	0.600	0.244	208	0.562	0.565	0.559

	8	0.600	0.367	145	0.392	0.401	0.397
	9	0.850	0.000	550	1.000	0.999	1.000
	10	0.850	0.122	400	0.727	0.708	0.734
	11	0.850	0.244	300	0.545	0.537	0.546
	12	0.850	0.489	123	0.224	0.233	0.226
	13	1.100	0.000	640	1.000	1	1.000
	14	1.100	0.122	456	0.713	0.716	0.728
	15	1.100	0.367	230	0.359	0.374	0.367
	16	1.100	0.489	134	0.209	0.221	0.210
	17	1.35	0.00	500	1.000	1.013	1.000
	18	1.35	0.24	385	0.770	0.774	0.764
	19	1.35	0.37	317	0.634	0.63	0.653
	20	1.35	0.49	250	0.500	0.481	0.529
	21	1.6	0.122	625	0.887	0.918	0.885
	22	1.6	0.244	528	0.749	0.755	0.761
	23	1.6	0.367	430	0.610	0.620	0.633
	24	1.6	0.489	333	0.472	0.471	0.502
	25	1.85	0.000	820	1.000	1.005	1.000
	26	1.85	0.122	725	0.884	0.889	0.880
	27	1.85	0.244	608	0.741	0.743	0.750
	28	1.85	0.367	490	0.598	0.607	0.615
	29	2.1	0.000	930	1.000	0.998	1.000
	30	2.1	0.122	810	0.871	0.860	0.875
	31	2.1	0.244	675	0.726	0.732	0.739
	32	2.1	0.489	382	0.411	0.451	0.455
	33	0.35	0.000	85	1.000	1.000	1.000
	34	0.35	0.147	63	0.741	0.714	0.714
	35	0.35	0.441	28	0.329	0.320	0.334
	36	0.35	0.588	13	0.153	0.155	0.169
	37	0.6	0.000	115	1.000	1.000	1.000
	38	0.60	0.29	58	0.504	0.495	0.491
	39	0.60	0.44	35	0.304	0.308	0.305
	40	0.60	0.59	16	0.139	0.146	0.133
	41	0.85	0.15	101	0.697	0.682	0.693
	42	0.85	0.29	70	0.483	0.477	0.477
	43	0.85	0.44	41	0.283	0.294	0.285
	44	0.85	0.59	19	0.131	0.138	0.108
	45	1.10	0.00	178	1.000	1	1.000

	46	1.10	0.15	121	0.680	0.673	0.687
	47	1.10	0.29	82	0.461	0.463	0.466
	48	1.10	0.44	47	0.264	0.281	0.270
	49	1.35	0.00	118	1.000	1.013	1.000
	50	1.35	0.15	106	0.898	0.903	0.868
	51	1.35	0.29	87	0.737	0.721	0.725
	52	1.35	0.59	52	0.441	0.397	0.427
	53	1.60	0.00	175	1.000	1.01	1.000
	54	1.60	0.15	154	0.880	0.874	0.861
	55	1.60	0.44	98	0.560	0.527	0.554
	56	1.60	0.59	70	0.400	0.392	0.394
	57	1.85	0.00	235	1.000	1.005	1.000
	58	1.85	0.29	165	0.702	0.698	0.695
	59	1.85	0.44	127	0.540	0.515	0.532
	60	1.85	0.59	89	0.379	0.386	0.365
	61	2.10	0.15	240	0.842	0.823	0.848
	62	2.10	0.29	194	0.681	0.686	0.683
	63	2.10	0.44	148	0.519	0.502	0.512
	64	2.10	0.59	103	0.361	0.381	0.338
Testing	65	0.350	0.000	276	1.000	1.000	1.000
	66	0.600	0.489	90	0.243	0.245	0.247
	67	0.850	0.367	210	0.382	0.387	0.380
	68	1.100	0.244	340	0.531	0.518	0.537
	69	1.35	0.12	450	0.900	0.946	0.892
	70	1.60	0.00	705	1.000	1.01	1.000
	71	1.85	0.489	370	0.451	0.461	0.478
	72	2.1	0.367	545	0.586	0.594	0.599
	73	0.35	0.294	44	0.518	0.511	0.513
	74	0.60	0.15	83	0.722	0.700	0.702
	75	0.85	0.00	145	1.000	0.999	1.000
	76	1.10	0.59	20	0.112	0.131	0.089
	77	1.35	0.44	69	0.585	0.540	0.578
	78	1.60	0.29	126	0.720	0.709	0.710
	79	1.85	0.15	202	0.860	0.846	0.854
	80	2.10	0.00	285	1.000	0.998	1.000

Table 2. Statistical values of parameters

Parameter	Maximum value	Minimum value	Average value	Standard deviation
d_f/B	2.1	0.35	1.225	0.572
α/ϕ	0.588	0	0.269	0.192
RF	1	0.112	0.638	0.264

Table 3. Connection weights and biases

Neuron	weight			Bias	
	w_{ik}		w_k	b_{hk}	b_0
	(d_f/B)	**(α/ϕ)**	***RF***		
Hidden neuron 1(k=1)	-0.1886	-1.5416	0.5663	0.6264	0.2388
Hidden neuron 2(k=2)	0.9381	3.8625	-0.2274	1.6575	
Hidden neuron 3(k=3)	13.1304	29.6581	-0.2938	31.5729	
Hidden neuron 4(k=4)	46.6441	-2.8076	0.3134	3.8462	

Table 4. Cross-correlation of the input and output for the reduction factor

Parameters	$\boldsymbol{d_f / B}$	$\boldsymbol{\alpha / \phi}$	$\boldsymbol{RF_{expt}}$
d_f / B	1	0	0.247
α / ϕ		1	-0.928
RF_{expt}			1

Table 5. Relative importance of different inputs as per Garson's algorithm and Connection weight approach

Parameters	**Garson's algorithm**		**Connection weight approach**	
(1)	Relative importance (%) (2)	Ranking of inputs as per relative importance (3)	S_i values as per connection weight approach (4)	Ranking of inputs as per relative importance (5)
d_f / B	38.86	2	10.44	2
α / ϕ	61.13	1	-11.34	1

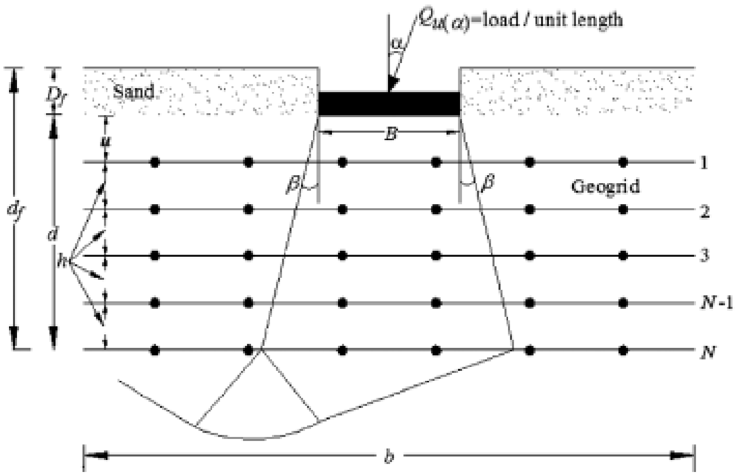

FIG. 1. Strip foundation over geogrid-reinforced soil subjected to inclined ultimate load

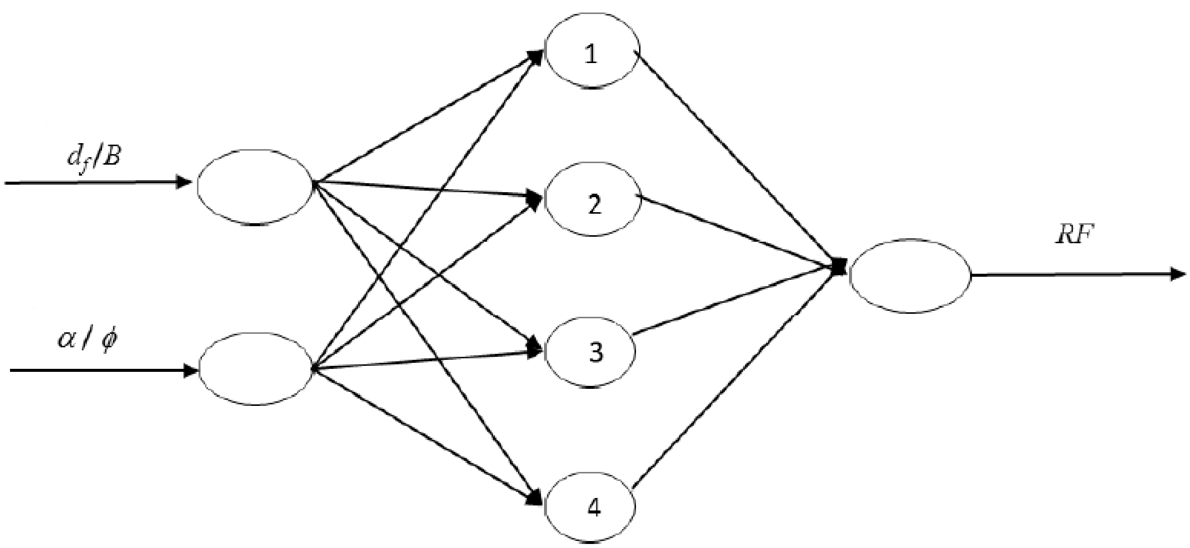

FIG. 2. Structure of ANN

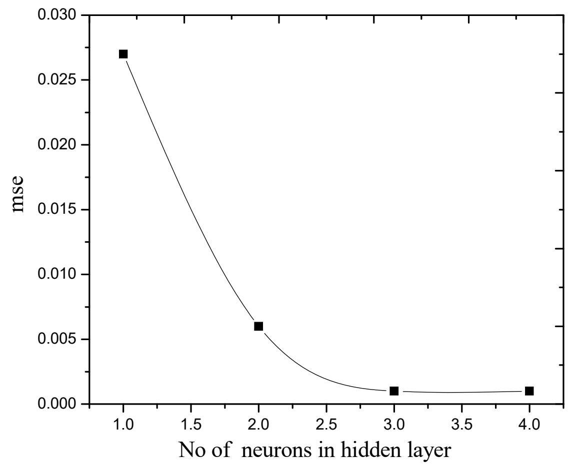

FIG. 3. Variation of hidden layer neuron with mean square error (mse)

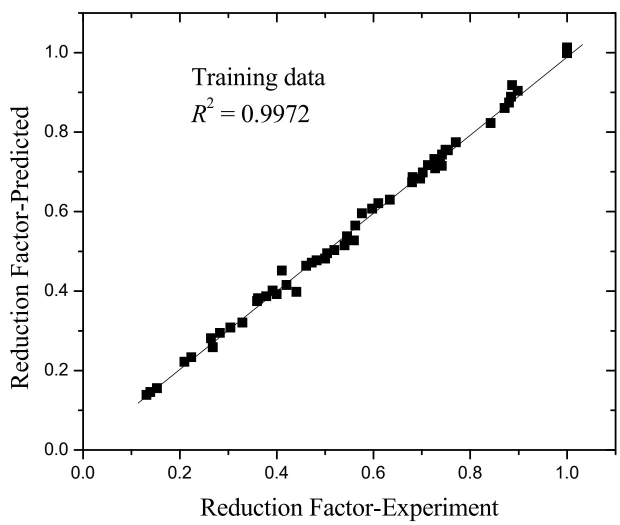

FIG. 4. Correlation between predicted reduction factor with experimental reduction factor for training data

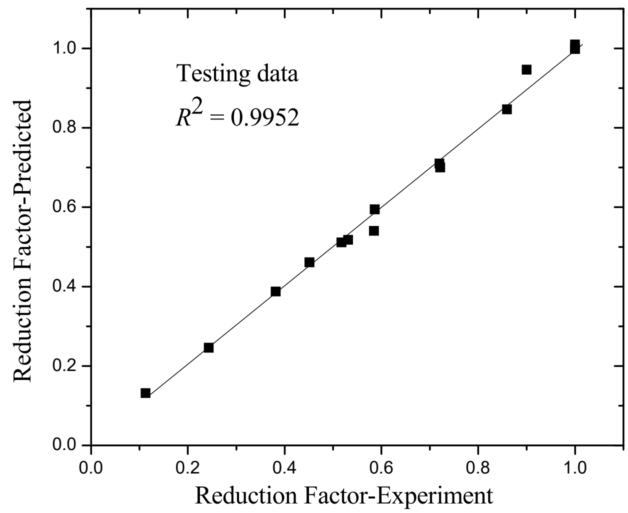

FIG. 5. Correlation between predicted reduction factor with experimental reduction factor for testing data

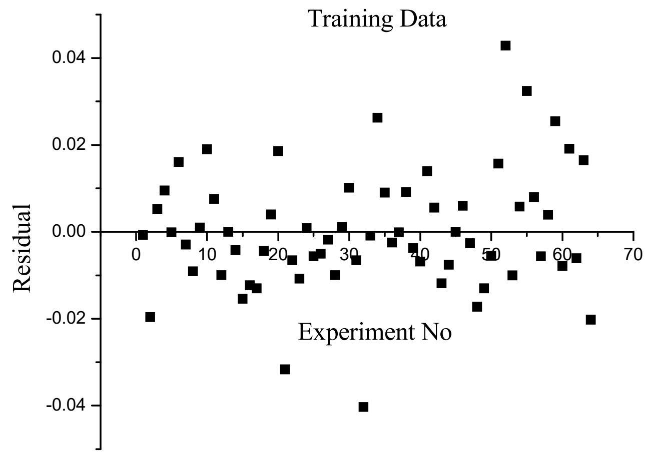

FIG. 6. Residual distribution of training data

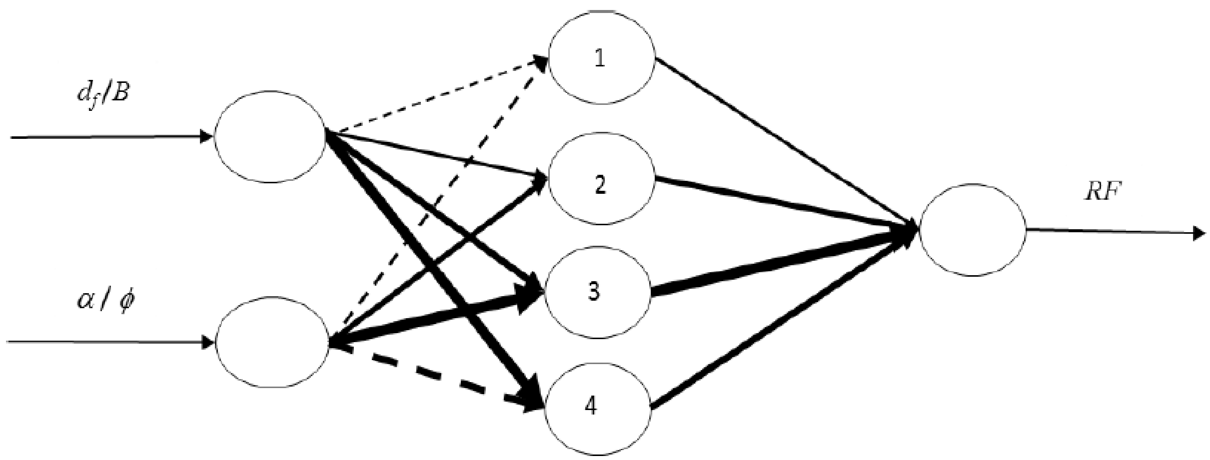

FIG. 7. Neural interpretation diagram showing lines representing connection weights and effects of inputs on reduction factor (RF)

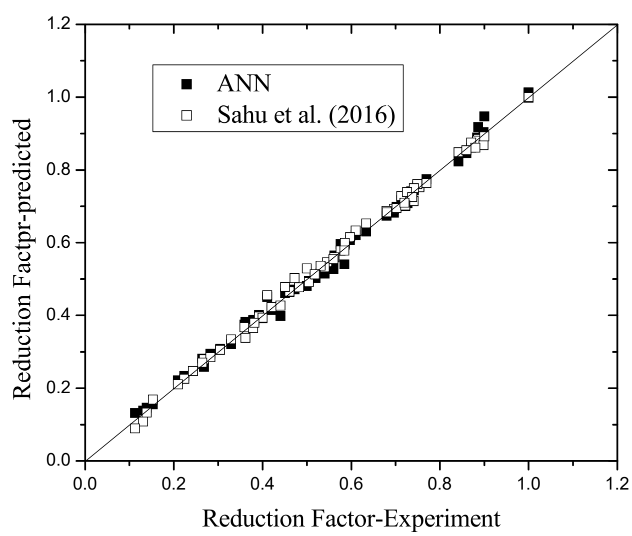

FIG. 8. Comparison of reduction factor of present analysis with empirical equation by Sahu *et al*. (2016)